




DETERMINING POINT SPREAD FUNCTION OF PRESSURE SENSITIVE LABELS FACESTOCK

Katarina Itrić Ivanda , Zrinka Jakopčević, Dorotea Kovačević ,
Suzana Pasanec Preprotić 

University of Zagreb, Faculty of Graphic Arts, Zagreb, Croatia

Abstract: Pressure sensitive labels (PSL) are a growing part of graphic industry. In the past, their design and application were rather limited to basic packaging and product information while currently labels are receiving more and more attention because they are customer's first contact with a product. PSL composition includes release liner, adhesive and facestock. Facestock can be considered as the most important part of the label since its properties determine the final label appearance. Nowadays, facestock material can be both paper and filmic. Therefore, it is necessary to perform a comprehensive characterization of pressure sensitive labels facestock in order to investigate the future impact of optical dot gain on the print. Point spread function is a measure of scattering and absorption of light in the given substrate. It carries information regarding paper composition and its future behaviour in term of optical dot gain. In the study, seven different facestock substrates were examined, two made from biogenic polyethylene, and five paper based PSL facestocks, three of which are made from 15% agro industrial waste by-products (barley, citrus and grape). Point spread function of the substrates were obtained by projecting collimated red laser light source on the facestock of pressure sensitive labels. Although the laser light used in this experiment was characterized by a narrow beam width of 0.5 mm and low divergence, <1 mrad, the beam was further converged and then passed through a space filter to ensure collimation of the laser beam which was then incident perpendicular to the set sample. Laser profile was firstly obtained by photodiode profiling. Based on the measured values of light intensity, the laser light profile was determined, as well as the average beam width that was needed for further image analysis. Image of the light scattering within the substrate was obtained perpendicular to the surface with Canon EOS 5DS camera. From the obtained image, laser profile was removed, and the resulting profile gives the point spread function of the substrate. The resulting images were processed with commercially available image analysis software (ImageJ). The mean background intensity subtracted from each individual pixel was determined to remove the background effect, and the distribution of the scattered light profile was achieved. The results showed that facestock composition has a high influence on PSF shape and width.

Key words: PSF, optical dot gain, pressure sensitive label, facestock, light scattering

1. INTRODUCTION

Pressure sensitive labels had come a long way since their first appearance in the 1930's until today. Their early design was based on a paper facestock, adhesive coating and a liner that was coated with silicone (Irwin, 1973). Nowadays the basic construction of the PSL is the same but the materials in use vary. For example, facestock can be made not only from paper but various polymer film materials such as PE, PP, PET, PVC, Polyvinyl Fluoride and Polyimide. Also, the adhesives can vary from solvent based, water-based, hot melt, UV hot melt, silicone-based. Each combination of facestock and adhesive is appropriate for specific storage conditions (temperature, humidity, exposure to chemicals and UV radiation). Of course, the mechanical and optical characteristics of the facestock surface like smoothness, mechanical resistance gloss, transparency, colour affect the overall print quality and durability of the printed label. Pressure sensitive label market is increasing rapidly in the last decade mainly because of the overall increase in distribution chain due to COVID. Consumer behaviour is changing, consequently the role of the labels too. Labels were initially used as an informative tool for product information, while nowadays their design significantly influences the buyer's decision about the product itself. Increasing the number of labels on the market also increases the amount of waste that needs to be disposed of. In this sense, it is necessary to include alternative materials to produce labels in order to use the various by-products that arise during the processing of different types of grain and fruits. This principle makes it possible to solve the problem of disposal of a large amount of organic waste through its utilization in paper and packaging industry. Cacao (Nurika, 2019), barley (Vargas et al., 2015), wheat (Tutus & Cicekler, 2016), pulp from

banana pseudo stem (Melesse et al., 2022), citrus (Tutus, Cicekler & Kucukbey, 2016) were all examined as a possible alternatives for paper production.

Characteristics of future print on PSL facestock made from such components is highly influenced by the characteristics of the PSL substrate itself. One of the ways of quantifying substrate is by determining its point spread function (PSF). PSF is a probability density function that describes the probability that a photon that entered the substrate exits on the same surface at a distance from the entry point. It is a measure of scattering and absorption of light in the given substrate since it carries information regarding PSL facestock composition and its future behaviour in term of optical dot gain. Importance of knowing the substrates point spread function is discussed in numerous articles since its shape and value is closely related to the optical dot gain.

Optical dot gain is caused by scattering of light within the paper (Rogers, 1998). Modrić et al. (2009) introduced the possibility of applying modified Monte Carlo model for characterizing optical dot gain by modelling light propagation within the paper based on its composition. Further research dealt with the Monte Carlo modelling of uncoated paper using randomly orientated microfacets. Modelling of the uncoated paper surface was based on paper surface reflectance data (Modrić, Maretić & Hladnik, 2012). The model was further improved in the case of coated papers by introducing photon behaviour at the interface between the coating and the rest of the paper (Modrić et al., 2013). During one of the steps, the photon can reach the border of the two media, such as in the predicted case the border between the coating and the rest of the paper, which is well defined. These layers can be considered as separate areas in which the optical properties differ significantly. This resulted with the determination of point spread function of paper substrate based on light-scattering simulation with the clear indication of Lorentzian function as the one that satisfactorily describes the shape of the PSF (Modrić, Maretić & Hladnik, 2014). Itrić et al. experimentally determined the PSF of the paper substrate and confirmed superiority of Lorentzian function for the description of the shape of the PSF, which was recently acknowledged by Rogers et al. (2019).

2. MATERIALS AND METHODS

2.1 Pressure sensitive labels facestock used in the study

For the purpose of analysing scattering of light within the PSL facestock comprised of different materials seven PSL of the same manufacturer were selected. In the selection of labels, care was taken to represent the most common paper-based labels, also included are those with a significant proportion of recycled fibres, as well as those based on synthetic polymers.

Two polymer bio based facestocks (polyethylene white-PEW and polyethylene clear-PEC) are primarily made from sugar cane ethanol. Its production is similar to one of conventional polyethylene and it is certified under the Bonsucro® layout and it is fully recyclable. It is characterized with a very high bio-based content (white minimum 80%, clear minimum 95%) (Avery Dennison Corporation, 2016; Avery Dennison Corporation, 2021). Chrome has a conventional filmic polymer facestock². Three fibre based facestocks used in this research are produced with 15% agro-industrial byproducts, 40% post-consumer recycled paper and 45% virgin wood pulp. Regarding different types of agro-industrial byproducts, citrus leftovers from juice production, grape pomace from wine production, and barley residue from whiskey production were used (Avery Dennison Corporation, 2021). Remaining fibre based facestock of thermal top is white woodfree, top coated thermal paper (Avery Dennison Corporation, 2022).

Table 1 (part 1): Properties of the used PSL facestocks given by the manufacturer ²⁻⁸

Sample name	Designation	Facestock	
		Basis weight ISO 536/g·m ²	Caliper ISO 534/ μm
Fasson® PE85 BIOB WHITE S692N-BG40WH FSC	PEW	82	82
Fasson® PE85 BIOB CLEAR S692N-BG40WH FSC	PEC	78	82
Fasson® THERMAL TOP K8 FSC R5100-BG40BR	TT	76	82
Fasson® 772 BRUSHED CHROME S697-HF125	CH	70	51

Table 1 (part 2): Properties of the used PSL facestocks given by the manufacturer ²⁻⁸

Fasson® rCRUSH CITRUS FSC S2030-BG45WH FSC	C	100	130
Fasson® rCRUSH BARLEY FSC S2030-BG45WH FSC	B	90	110
Fasson® rCRUSH GRAPE FSC S2047N-BG45WH IMP FSC	G	90	114

2.2 Procedure of obtaining PSF

When determining the PSF, the linearity of the input-output system is assumed (Dainty & Shaw, 1974), whereby $f(x,y)$ represents input, and $g(x,y)$ output, while the operation of the system is represented by the operator $S\{ \}$, and it is valid then

$$g(x,y) = S\{f(x,y)\} \quad g(x, y) = S\{f(x, y)\} \quad (1)$$

If the input information is described as

$$f(x, y) = \iint_{-\infty}^{+\infty} f(x', y') \delta(x - x') \delta(y - y') dx' dy' \quad (2)$$

$$f(x, y) = \iint_{-\infty}^{+\infty} f(x', y') \delta(x - x') \delta(y - y') dx' dy' \quad f(x, y) = \iint_{-\infty}^{+\infty} f(x', y') \delta(x - x') \delta(y - y') dx' dy'$$

And the output is defined as

$$g(x, y) = S\left\{\iint_{-\infty}^{+\infty} f(x', y') \delta(x - x') \delta(y - y') dx' dy'\right\} \quad (3)$$

$$g(x, y) = S\left\{\iint_{-\infty}^{+\infty} f(x', y') \delta(x - x') \delta(y - y') dx' dy'\right\}$$

due to the linearity of the system it can be shown that

$$g(x, y) = \iint_{-\infty}^{+\infty} f(x', y') S\{\delta(x - x') \delta(y - y')\} dx' dy' \quad (4)$$

$$g(x, y) = \iint_{-\infty}^{+\infty} f(x', y') S\{\delta(x - x') \delta(y - y')\} dx' dy'$$

where the system response is the so-called point spread function (PSF).

$$H(x, x'; y, y') = S\{\delta(x - x') \delta(y - y')\} \quad H(x, x'; y, y') = S\{\delta(x - x') \delta(y - y')\} \quad (5)$$

Method of determining PSF was developed in 2017. by Itrić et. al. (2017) and is presented in Fig. 1. The method itself comprises of laser profile energy distribution measurement followed by scattered light intensity of substrate. Laser used in the research was helium-neon red laser with the beam diameter of 0.5 mm, output wavelength of 632.8 nm and beam divergence ≤ 1 mrad. Spatial filter in the form of the 350 μm was placed in front of the laser on the optical bench in order to secure spatial coherence. Also, optical lens, 10 cm focal length, was added as a condenser. At the other edge of the optical bench, single photodiode was mounted for efficient laser profiling. Photodiode possesses its own transconductance amplifier in the desired spectral range and a high signal to noise ratio along with a slit diaphragm for high resolution light intensity measurements. Average laser profile was plotted in Origin 9 mathematical software. The exact width of the laser beam was determined so it can be subtracted in the following step.

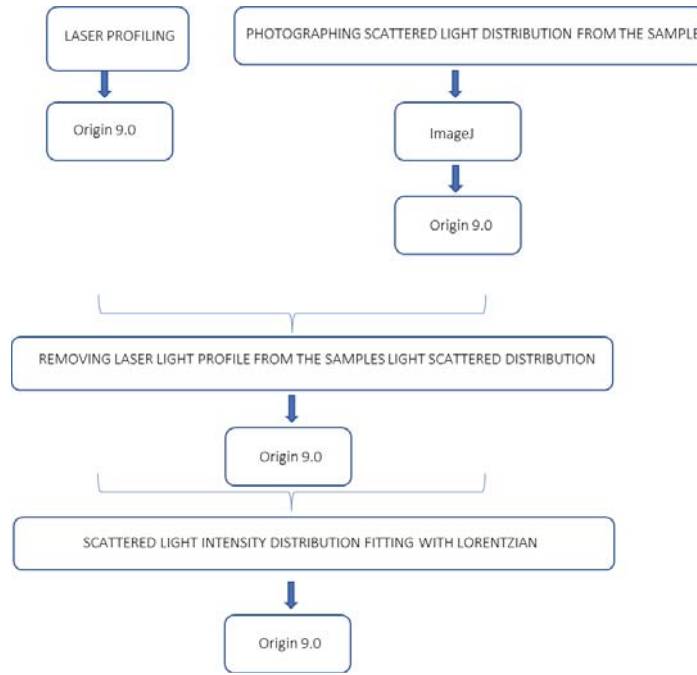


Figure 1: Procedure of generating PSF

Scattered light intensity of the laser on the facestock substrate was obtained by photographing the resulting interference of point light source with the substrate perpendicular to the substrate itself. Deviations of up to 2 degrees are possible. The Canon XC10 4K camera with 50 mm, 1/30 sec at f 5.6, ISO 400 was used for the imaging of the samples. ImageJ software was used for further image processing. Recorded image profiles of subsurface light scattering showed cylindrical symmetry which is why the mean value of the vertical and horizontal profiles was chosen for a reliable profile analysis. Final scattering distribution was obtained by removing the laser light profile. Resulting profile was normalized to unity and fitted with Lorentzian function in Origin 9 according to eq. 6.

$$y = y_0 + \frac{2A}{\pi} \cdot \frac{w}{4(x-x_c)^2+w^2} y = y_0 + \frac{2A}{\pi} \cdot \frac{w}{4(x-x_c)^2+w^2} \quad (6)$$

Lorentzian function is 4 parameter function, where y_0 stands for the offset of the function, x_c is the position of the centre, w is full width at half maximum (FWHM) and A is the area under the curve.

3. RESULTS AND DISCUSSION

Resulting experimental PSFs are presented in Figure 1. Every PSF was fitted with Lorentzian function in order to acquire numerical quantities that can be further used as a prediction parameters of optical dot gain. Upper two thirds of all experimentally acquired PSFs are uniform and symmetric while at the wings the influence of the noise arises resulting in irregularities and greater deviations from the proposed model function.

All of the fitted PSF show satisfactory correlation with the Lorentzian PSF, $R^2 > 0.96$ (Table 2). If higher level of smoothing was used the correlation would be even higher. It was estimated that this level of correlation is adequate to achieve the ideal ratio of level of smoothing and preservation of background information. The wings of the PEC point spread function are flatter compared to PEW facestock PSF (Figure 1 a-b).

Table 2: Correlation of Lorentzian PSF with the measured PSF

Designation	PEC	PEW	TT	CH	C	B	G
R ²	0.97365	0.98185	0.967	0.9839	0.985	0.98252	0.9712

By fitting the measured PEC PSF with Gaussian, 0.99 correlation was obtained. This is an indication of approximating clear filmic based PSF with the Gaussian function, while the paper based and filmic with the addition of white pigment is better described by Lorentzian. Obviously, the interaction of light with the clear bio based polymer results in different behaviour compared to paper substrates, in terms of the shape of the line spread function.

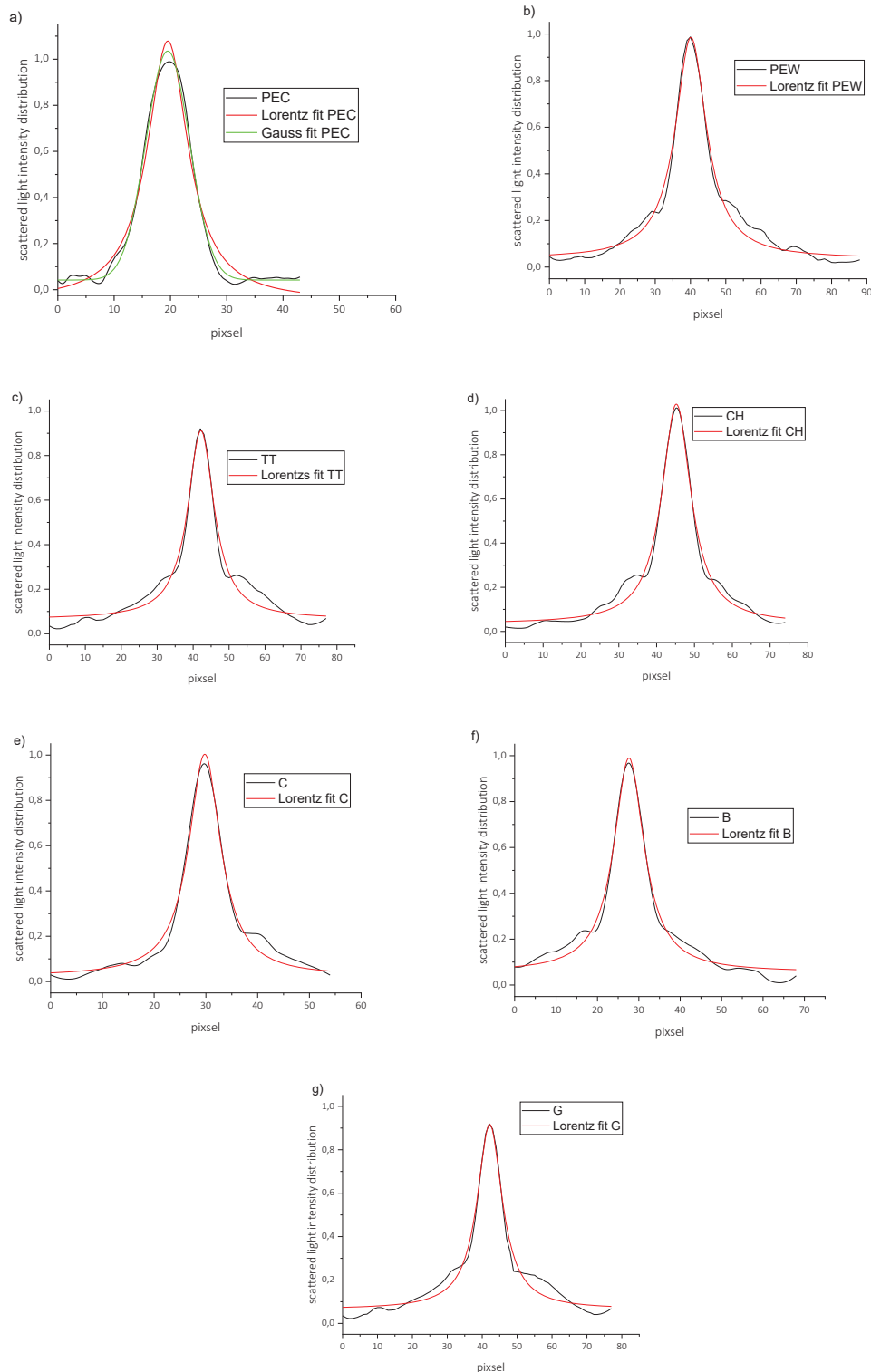


Figure 2: Measured and fitted PSL facestock point spread functions of a) polyethylene clear, b) polyethylene white, c) thermal top, d) chrome, e) citrus, e) barley, f) grape

Numerical parameters, w , A , y_0 and x_c of the fitted Lorentzian PSFs are given in Table 2.

Table 3: Values of the Lorentzian parameters used to fit PSL facestock point spread function Correlation of Lorentzian and Gaussian with the measured data

Designation	w	A	y_0	x_c
PEC	$8.84216 \pm 0,47652$	$15.67975 \pm 0,82142$	-0.04996 ± 0.01656	19.53018 ± 0.11683
PEW	10.73371 ± 0.32068	16.01006 ± 0.41002	0.03564 ± 0.00529	40.11795 ± 0.09205
TT	8.91329 ± 0.38728	11.84832 ± 0.43685	0.06575 ± 0.0066	42.1703 ± 0.11251
CH	9.4092 ± 0.28854	14.70078 ± 0.38865	0.03453 ± 0.00583	45.21705 ± 0.08253
C	7.52866 ± 0.26449	11.59962 ± 0.35843	0.02294 ± 0.00702	29.77081 ± 0.07364
B	8.90319 ± 0.29813	13.06042 ± 0.37943	0.05589 ± 0.0061	27.62036 ± 0.08456
G	8.77083 ± 0.35514	11.73341 ± 0.40198	0.06508 ± 0.00613	42.15353 ± 0.10352

Chemical composition obtained by FTIR in our previous research (Vukoje et al., 2021) confirmed the same composition of the PEW and PEC which is also stated in their product sheet (Avery Dennison Corporation, 2021). Nevertheless, their PSF differ. The scattering coefficient of polymer is ruled by the polymer matrix and different additives used for enhancing desirable polymer properties. Every additive has its own refractive index. The higher the difference between refractive indices of the components the higher scattering of light occurs. Addition of white pigment into the polyethylene base clearly caused the increase in light scattering, resulting in highest full width at half maximum.

From paper based PSL facestock, the one comprising of 15 % citrus byproducts from orange juice production shows the lowest value of FWHM indicating least scattering of the incident light. Due to the fact that all three paper based facestocks with 15% ratio of byproducts from citrus, grape and barley have the same amount of recycled and virgin fiber, the differences in the PSF width corresponds to the fibre characteristics of depectinized micronized citrus mash, barley and grape pomace. Citrus pulp contains 128 g/kg of cellulose fibres, together with 183 g/kg hemicellulose. On the other hand, grape pomace has 540 g/kg of cellulose fibres and 208 g/kg of hemicellulose. The lignin content in grape pomace is higher than that in citrus pulp 197 g/kg compared to 22 g/kg (Mussatto, Dragone & Roberto, 2006) indicating the higher level of chemical bleaching that had to be applied. As for barley fibres, research by Mossatto et. al. (2006) showed that chemical composition of exhausted barley malt consists of 25.4 % cellulose and 11.9 % of lignin.

Thermal top PSL facestock shows the widest FWHM from all paper based facestocks which can be explained with the existence of coating. Namely, it is well known that the lateral light scattering is more pronounced within coated papers due to numerous interactions between the coating layer and the substrate. Filmic based facestock, CH, confirms higher level of scattering of light within the filmic PSL facestocks. Due to its lower weight compared to PEW and PEC PSL facestock the scattering of light is lower and consequently the point spread function is narrower.

This data can be indicative for the evaluation of the future print characteristics. In the research that dealt with determining the quality of the printed monochrome line of 0.5 pt nominal width on PSL facestocks examined in this study, it was observed that dot gain, including both mechanical and optical dot gain was lower for paper based PSL facestocks (Itrić et al., 2022).

4. CONCLUSIONS

The demand for an attractive PSL design is more and more pronounced. Therefore, the need for the characterization of such substrates increases in order to obtain as many measurable values as possible that can give useful information and which can be used for future prediction of print quality. One of the values that affects this is optical dot gain. Optical dot gain or lateral scattering of light within the substrate can be characterized by point spread function.

Pressure sensitive labels consist of liner, adhesive and facestock. In the research we examined the possibility of applying previously developed method for determining point spread function of paper substrate based on laser-paper substrate interaction for determining point spread function of PSL facestock. The method is based on image analysis since the laser-substrate interaction is captured with

the camera and further processed in image processing software ImageJ followed by the mathematical fitting in Origin 9. Red laser was used to gain the highest levels of lateral light scattering within the samples due to its wavelength. Both types of facestock material, paper and filmic, were represented. Paper facestock was represented by four label types, three of which are with a high percentage of agro-industrial byproducts, barley, citrus and grape, while the fourth is wood-free coated paper. Filmic PSL facestocks are represented with two bio based PSL facestocks, PEW and PEC, made from sugar cane and one conventional polymer based, TT.

Results showed that measured PSFs of all PSL facestocks can be satisfactorily fitted by means of Lorentzian function. Also, paper based PSL facestock shows lower level of light scattering compared to filmic ones. It should be also noted that coated paper based PSL facestock, TT, has the widest PSF FWHM value. This is supported with the fact that coating increases the degree of reflections and scattering between the substrate and the coating layer.

The results showed that facestock composition has a high influence on PSF shape and width. The research confirmed that in terms of the shape and properties of the point spread function of the ecology friendly facestock made from a significant ratio of industrial by products is compatible to the commercial woodfree PSL facestock.

5. ACKNOWLEDGMENTS

This research is supported by University of Zagreb short term funding.

6. REFERENCES

AveryDennison Corporation. (2016) *Bio-based PE Film - A sugar-sweet opportunity, product overview*. Available from:

https://www.averydennison.com/content/dam/averydennison/lpm/ap/en_cn/doc/home/news-and-events/tradeshows/BioCane_PE_EN.pdf [Accessed 5th April 2022]

AveryDennison Corporation. (2022) *Fasson Brushed Chrome*. Available from:

<https://www.pds.averydennison.com/content/PDS/AA659> [Accessed 5th April 2022]

AveryDennison Corporation. (2021) *Fasson PE85 BIOB CLEAR S692N-BG40WH FSC PE85*. Available from:

<https://www.pds.averydennison.com/content/PDS/BC449> [Accessed 5th April 2022]

AveryDennison Corporation. (2021) *Fasson PE85 BIOB WHITE S692N-BG40WH FSC PE85*. Available from:

<https://www.pds.averydennison.com/content/PDS/BC449> [Accessed 5th April 2022]

AveryDennison Corporation. (2021) *Fasson rCRUSH BARLEY FSC S2030-BG45WH FSC*. Available from:

<https://www.my-muse.com/en/home/insights/the-graduate-collection/fasson-rcrush-barley-fsc.html> [Accessed 5th April 2022]

AveryDennison Corporation. (2021) *Fasson rCRUSH CITRUS FSC S2030-BG45WH FSC*. Available from:

<https://www.pds.averydennison.com/content/PDS/AE294?UL=4> [Accessed 5th April 2022]

AveryDennison Corporation. (2021) *Fasson rCRUSH GRAPE FSC S2047N-BG45WH IMP FSC*. Available from:

<https://www.my-muse.com/en/home/materials/eu16-rcrush-grape-fsc.html> [Accessed 5th April 2022]

AveryDennison Corporation. (2022) *Fasson Thermal Top*. Available from:

<https://www.pds.averydennison.com/content/PDS/AP764?UL=1> [Accessed 5th April 2022]

Dainty, J. C. & Shaw, R. (1974) *Image science : principles, analysis and evaluation of photographic-type imaging processes*. London, Academic Press

Irwin R. (1973) Development of Pressure-sensitive labels. *Adhesive age*. 16 (12).

Itrić Ivanda, K., Jakopčević, Z., Vukoje, M. & Kulčar, R. (2022) QUALITY OF THE LINE REPRODUCTION ON ENVIRONMENTALLY FRIENDLY PRESSURE SENSITIVE LABELS FACESTOCK. In: Çınar, Ö. (ed.) *8th International Conference on Sustainable Development, 04 - 08 May, Sarajevo*. p. 5

- Itrić, K., Modrić, D. & Hladnik, A. (2017) A novel method for determining the optical component of the paper substrate point spread function. *Optik*. 140, 555-564. Available from: doi: 10.1016/j.ijleo.2017.04.090
- Melesse, E. Y., Bedru, T. K. & Meshesha, B. T. (2022) Production and Characterization of Pulp from Banana Pseudo Stem for Paper Making Via Soda Anthraquinone Pulping Process. *International Journal of Engineering Research in Africa*. 58, 63–76.
- Modrić, D., Bolanča, S. & Beuc, R. (2009) Monte Carlo modeling of light scattering in paper. *Journal of Imaging Science and Technology*. 53 (2), 0202011-0202018
- Modrić, D., Maretić, K. P. & Hladnik, A. (2012) Modeling spatial reflection from an uncoated printing paper using Monte Carlo simulation. *Nordic Pulp & Paper Research Journal*. 27 (5), 968–975. Available from: doi: 10.3183/NPPRJ-2012-27-05-p968-975
- Modrić, D., Petric Maretić, K. & Hladnik, A. (2014) Determination of point-spread function of paper substrate based on light-scattering simulation. *Applied Optics*. 53 (33), 7854 - 7862. Available from: doi:10.1364/AO.53.007854
- Modrić, D., Petric Maretić, K. & Itrić, K. (2013) Modeliranje podpovršinskog raspršenja fotona u papiru Monte Carlo simulacijom. *Tehnički glasnik*. 7(4), 337–343.
- Mussatto, S. I., Dragone, G. & Roberto, I. C. (2006) Brewers' spent grain: Generation, characteristics and potential applications. *Journal of Cereal Science*. 43 (1), 1–14. Available from: doi: 10.1016/j.jcs.2005.06.001
- Nurika, I. (2019) The pattern of lignocellulose degradation from Cacao pod using the brown rot (*Serpula lacrymans*) and white rot (*Schizophyllum commune*) fungi. *IOP Conference Series: Earth and Environmental Science*. 230 (1), 1-8. Available from: doi: 10.1088/1755-1315/230/1/012080
- Rogers, G., Corblet, O., Fournel, T. & Hebert, M. (2019) Measurement of the diffusion of light within paper. *Journal of the Optical Society of America A*. 36 (4), 636–640. Available from: doi: 10.1364/JOSAA.36.000636
- Rogers, G. L. (1998) Measurement of the modulation transfer function of paper. *Applied optics*. 37 (31), 7235–7240. Available from: doi: 10.1364/AO.37.007235
- Tayengwa, T. & Mapiye, C. (2018) Citrus & Winery Wastes: Promising Dietary Supplements for Sustainable Ruminant Animal Nutrition, Health, Production, and Meat Quality. *Sustainability*. 10 (10), 3718. Available from: doi:10.3390/su10103718
- Tutuş, A. & Çiçekler, M. (2016) Procjena mogućnosti upotrebe strnjike obične pšenice (*Triticum aestivum* L.) za proizvodnju celuloze i papira. *Drvena Industrija*. 67 (3), 271–279. Available from: doi:10.5552/drind.2016.1603
- Tutuş, A., Cicekler, M. & Kucukbey, N. (2016) Pulp and Paper Production from Bitter Orange (*Citrus aurantium* L.) Woods with Soda-AQ Method. *KASTAMONU UNIVERSITY JOURNAL OF FORESTRY FACULTY*. 16 (1),14–18.
- Vargas, F., González, Z., Rojas, O., Garrote, G. & Rodríguez, A. (2015) Barley straw (*Hordeum vulgare*) as a supplementary raw material for *Eucalyptus camaldulensis* and *Pinus sylvestris* kraft pulp in the paper industry. *BioResources*. 10 (2), 3682–3693. Available from: doi:10.15376/biores.10.2.3682-3693
- Vukoje, M., Itrić Ivanda, K., Kulčar, R. & Marošević Dolovski, A. (2021) Spectroscopic Stability Studies of Pressure Sensitive Labels Facestock Made from Recycled Post-Consumer Waste and Agro-Industrial By-Products. *Forests*. 12 (1703), 1–15. Available from: doi: <https://doi.org/10.3390/f12121703>



© 2022 Authors. Published by the University of Novi Sad, Faculty of Technical Sciences, Department of Graphic Engineering and Design. This article is an open access article distributed under the terms and conditions of the Creative Commons Attribution license 3.0 Serbia (<http://creativecommons.org/licenses/by/3.0/rs/>).

